PICOSECOND AND STEADY STATE, VARIABLE INTENSITY AND VARIABLE TEMPERATURE EMISSION SPECTROSCOPY OF BACTERIORHODOPSIN

S. L. SHAPIRO AND A. J. CAMPILLO, *University of California, Los Alamos Scientific Laboratory, Los Alamos, New Mexico 87545,*
A. LEWIS, G. J. PERREAULT, J. P. SPOONHOWER, AND R. K. CLAYTON, *Cornell University, Ithaca, New York 14850,* AND
W. STOECKENIUS, *Department of Biochemistry and Biophysics, University of California, San Francisco, California 94143 U. S. A.*

ABSTRACT The bacteriorhodopsin emission lifetime at 77°K has been obtained for different regions of the emission spectrum with single-pulse excitation. The data under all conditions yield a lifetime of 60±15 ps. Intensity effects on this lifetime have been ruled out by studying the relative emission amplitude as a function of the excitation pulse energy. We relate our lifetime to previously reported values at other temperatures by studying the relative emission quantum efficiency as a function of temperature. These variable temperature studies have indicated that an excited state with an emission maximum at 670 nm begins to contribute to the spectrum as the temperature is lowered. Within our experimental error the picosecond data seem to suggest that this new emission may arise from a minimum of the same electronic state responsible for the 77°K emission at 720 nm. A correlation is noted between a 1.0-ps formation time observed in absorption by Ippen et al. (Ippen, E. P., C. V. Shank, A. Lewis, and M. A. Marcus. 1978. Subpicosecond spectroscopy of bacteriorhodopsin. *Science* [*Wash. D.C.*]. **200**:1279–1281 and a time extrapolated from relative quantum efficiency measurements and the 77°K fluorescence lifetime that we report.

Because of its remarkable properties, the purple membrane of *Halobacterium halobium* has attracted much interest. The membrane contains a single protein which was called bacteriorhodopsin (1, 2) because of certain similarities with rhodopsin—the primary light absorber and initiator of the visual process. Bacteriorhodopsin, like rhodopsin, is composed of lipid and protein complexed via a protonated Schiff base linkage (3) to an all-*trans* retinal chromophore, and this probably accounts for the many spectral similarities between these proteins.

Oesterhelt and Stoeckenius (2) have shown that bacteriorhodopsin acts as a light-driven proton pump, and kinetic resonance Raman spectroscopy has demonstrated (4) that light causes the deprotonation of the Schiff base proton in 10–30 μs. Thus, the chromophore is directly involved in both the primary and subsequent events in the proton pumping cycle. Therefore, it is important to understand the primary photo-

physical phenomena in the chromophore that are associated with this conversion of light energy into a proton gradient.

Stoeckenius and Lozier (5) and Lozier et al. (6) were the first to show that absorption of a photon by bacteriorhodopsin (bR_{570}) λ_{max} = 570 nm leads to a molecular species with a red-shifted absorption called K_{610}. This red-shifted species exhibits a maximum at 615 nm in its difference spectrum with bR_{570}. Kaufmann et al. (7) have observed rapid formation ($\leq$6 ps) of this intermediate in bacteriorhodopsin's photochemical cycle after excitation with a picosecond light pulse (apparently formed analogously to a "red-shifted" state in rhodopsin [8]). It can be shown that in both rhodopsin and bacteriorhodopsin this "red-shifted" species is at higher energy than the respective parent pigments (9, 10); recently, subpicosecond techniques have allowed Ippen et al. (11) to measure the formation time of this intermediate to be 1.0±0.5 ps.

The observation by Lewis et al. (12) of light emission from bacteriorhodopsin has opened up the possibility of using fluorescence studies to learn more about the initial steps in the biological energy conversion process. Because the fluorescence lifetimes are short, picosecond techniques must be used for their measurement. Alfano et al. (13), though unable to directly measure the fluorescence lifetime at room temperature, estimated the lifetime to be 3 ps by using a Kerr gate technique. A time-resolved lifetime of 40 ps at 90°K was also reported by this group. Hirsch et al. (14) have reported the fluorescence lifetime at room temperature to be 15 ps by using an up-conversion gate. Both groups used pulse-train excitation, with 100–1,000 pulses incident on the sample.

Our main purpose is to present measurements of the fluorescence lifetime at 77°K in bacteriorhodopsin accomplished with *single*-pulse excitation and a streak camera detection technique. By avoiding complications possible with multiple-pulse excitation, such a single-pulse fluorescence measurement clarifies the situation. Also, to correlate our lifetime at 77°K with the lifetimes of Alfano et al. (13) and Hirsch et al. (14) at other temperatures, we have recorded the spectrum of the emission and evaluated the quantum yield as a function of temperature. The temperature dependence of the emission shows a population of emitting state/states that may not necessarily contribute to the room temperature emission. We demonstrate that our lifetime data at 77°K are compatible with the 1-ps evolution time of K_{610} as measured by Ippen et al. (11) and the 40-ps, 90°K emission lifetime of Alfano et al. (13). Finally, to avoid misinterpretations in our analysis because of possible errors that can appear at high intensities, we have also investigated primary processes in bacteriorhodopsin as a function of these high intensities, and these data are also reported.

MATERIALS AND METHODS

Temperature Dependence of the Emission Quantum Efficiency

Bacteriorhodopsin, in the form of purple membrane fragments, was prepared by procedures described elsewhere (15). The fragments were sonicated (using a Fisher Ultrasonic probe; Fisher Scientific Co., Pittsburgh, Pa.) to produce a uniform particle size. The reduction of size

of the particulate matter minimizes problems due to scattering. The membrane fragments (OD = 1.0) were buffered to pH 5.0 with 0.1 M sodium acetate.

In the low temperature experiments, water-washed purple membrane fragments, pH 5.0, were suspended in a glycerol-water mixture (roughly 3/1 vol/vol), and 1.0-mm path length cells containing samples (OD = 0.3) were used. In the room temperature experiments, the amount of light absorbed by the sample in question was determined by the use of a Yellow Springs-Kettering radiometer model 65 (Yellow Springs Instrument Co., Yellow Springs, Ohio). The scattering contribution to the observed bacteriorhodopsin spectra was estimated by recording the spectrum of a silica gel suspension. The concentration of the silica gel sample was adjusted to match the scattering of bacteriorhodopsin at 1,000 nm.

The choice of an emission standard for the measurement of small quantum efficiencies requires careful consideration. We chose photosynthetic reaction centers isolated from the bacterium *Rhodopseudomonas sphaeroides* (16) because, like bacteriorhodopsin, they also emit in the near-infrared region and their emission efficiency is relatively small (17). The reaction centers were rendered photochemically inactive by adding $Na_2S_2O_4$. Thus, errors in correcting for frequency response of the fluorometer and errors associated with attempting to compare a weakly emitting species with a strongly emitting species are reduced.

The emission quantum efficiencies were measured with a spectrometer using a 450 W high-pressure xenon arc lamp for excitation and an RCA 7102 photomultiplier (RCA Solid State, Somerville, N.J.) cooled with dry ice for detection. The exciting light was passed through a Zeiss flint prism monochromator, operated with half bandwidth 4–20 nm in the range of 400–600 nm, then through 5 cm of water, an optical filter, and finally onto the sample. Emission was collected at 90° to the axis of excitation; it passed through optical filters and a Bausch and Lomb 0.5-m grating monochromator (half bandwidth 15 nm; Bausch & Lomb Inc., Rochester, N.Y.) before reaching the photomultiplier. When measuring emission spectra, the optical filters were a 500-nm broad band interference filter in the excitation path and a Corning 2-73 filter (Corning Glass Works, Corning, N.Y.) in the measuring path. The photocurrent was delivered to an electrometer amplifier whose output was recorded and in some cases processed with a Tracor Northern TN-1500 signal averager (Tracor Northern, Middleton, Wisc.). The aperture of the optical system was $f/6$ for both excitation and detection. The sensitivity of the measuring system as a function of wavelength was calibrated by recording the emission spectrum of a tungsten lamp, treated as a blackbody at 2,860°K. For measurements at room temperature, the sample was held in a quartz cell, 1 × 1 × 4 cm high. For measurements at temperatures down to 40°K, the sample was held in a flat quartz cell, 1.0 mm path, oriented about 45° to both exciting and measuring axes. This cell was attached to the cold probe of a closed cycle helium refrigerator (Cryogenic Technology Inc., Waltham, Mass.). Absorption spectra were measured with a Cary 14R spectrophotometer (Cary Instruments, Varian Associates, Palo Alto, Calif.) to monitor the presence of intermediates which could alter the bacteriorhodopsin concentration and cause errors in the emission quantum efficiency measurements.

Temperature Dependence of Emission Band Profiles

A sonicated suspension of bacteriorhodopsin in doubly distilled water (absorbance = 4.5 for 1-cm path length) was placed in a 1.0-mm path length quartz cell attached to the cold head of a Spectrim cryostat (Lake Shore Cryotronics, Inc., Eden, N.Y.). After exposure to room lights during preparation and insertion in the cryostat, the sample was kept in the dark for 5 min before cooling to 17°K. This procedure allows any intermediates to convert to bR_{570} (light-adapted bacteriorhodopsin), but does not form the dark-adapted bR_{560}. The temperature equilibrated at 17°K within 1.5 h. The spectra were then acquired at a sequence of increasing temperatures, except for a return to 17°K between the 100° and 150°K spectra. The band

shape at 17°K was repeatable. At least 1 h was allowed for equilibration at each new temperature. Emission was monitored at a fixed wavelength (14,300 or 15,100 cm^{-1}) to monitor the equilibration process. As a further check of repeatability, at least two spectra were taken at each temperature (except at 200°K).

Data were collected on a Raman spectrometer, much as reported previously (12). The excitation power was 5 mW at 514.5 nm (19,435 cm^{-1}) from a Coherent radiation model 52B argon ion laser (Coherent Inc., Palo Alto, Calif.). Although no preillumination at other wavelengths was used, our fluorescence spectra in the 680-nm region at 77°K obtained with xenon arc excitation was identical to spectra obtained at similar wavelengths and temperatures with laser excitation. This is particularly important because the results of Gillbro et al. (18) indicated that laser excitation may affect the emission in this region. We, on the other hand, as will be discussed below, have observed temperature-dependent effects in this region which may account for the discrepancies observed by Gillbro et al. (18).

The emitted light was collected, collimated, and focused by two lenses in a backscattering arrangement, dispersed by a Spex 1401 double monochromator (Spex Industries, Inc., Metuchen, N.J.), and detected using an RCA C31034 photomultiplier (RCA Solid State) connected to digital photon counting electronics described previously (19). The monochrometer step size was 10 cm^{-1}, with a counting time of 5 or 10 s per channel. The slits were set for 1 or 4 cm^{-1} resolution, as necessary for good signal-to-noise ratio.

The spectra were processed and plotted using a system of programs developed on a MODCOMP II/221 minicomputer system. Correction for instrument response is accomplished by dividing by the response as previously determined using a standard tungsten lamp (Optronics International, Inc., Chelmsford, Mass.). After correction, the spectra were compressed to a 50 cm^{-1} effective step size and smoothed using a 7-point cubic polynomial-fitting convolute (20). This procedure smooths the shot noise away without appreciably distorting features with half-width greater than 350 cm^{-1}.

The plots represent photons emitted per unit frequency interval as a function of frequency in cm^{-1}. This is important to note because peak locations are not generally identical to those for a wavelength axis. In the plot, the areas are normalized to a constant; this facilitates comparison of structures of spectra whose overall magnitudes are strong functions of temperature.

Emission Lifetime and Variable Intensity Measurements

The system for measuring the relative quantum yields at high intensities and the fluorescence lifetimes has been described previously (21, 22). A single pulse is selected from a modelocked Nd:YAG (neodymium:yttrium aluminum garnet) laser pulse train, is wavelength shifted to 530 nm by passage through a KDP (potassium dihydrogen phosphate) crystal, and imaged spatially onto the sample by appropriate mechanics and optics. The fluorescence is collected onto the slit of a streak camera, the phosphorescent streak is projected onto an optical multichannel analyzer, and the information is displayed on an oscilloscope so that the lifetime may be recorded on a single shot. The energy of the pulse is measured with an energy meter; for relative quantum yield measurements the fluorescence is detected with a photomultiplier. Both S-1 and S-20 response streak tubes were used to measure the fluorescence lifetimes, and the results from the two tubes were consistent.

To test for nonlinear effects the incident laser intensity may be varied with nonsaturable filters. The laser intensity on the sample may be increased by removing an attenuator from the beam path to the sample. If the filter is then placed between the sample and/or the streak camera or photomultiplier, calibration errors may be minimized. Because the emission spectra of bacteriorhodopsin cover a wide range, to calibrate the filter transmission accurately it is sometimes necessary to insert narrow band pass filters before the photomultiplier to select fluorescence wavelength intervals.

Samples were prepared by the method of Oesterhelt and Stoeckenius (15). The light-adapted sample was contained in a 1-mm path-length cuvette, and absorption was about 90% depending on the sample. For quantum yield measurements the absorption was limited to small values, 7–17%, to minimize corrections resulting from variations in intensity due to Beers law. For picosecond fluorescence lifetime measurements the absorption must be kept high to avoid time-delay effects associated with sample length.

The excitation pulse width as measured by our Electrophotonics (Electrophotonics, Belfast, Northern Ireland) ICC-512 streak camera was 25 ps. A Corning 2–58 filter (Corning Glass Works) was placed between the sample and the streak camera to eliminate scattered laser light. For measuring the lifetimes of the two emission bands at 77°K, narrow band filters corresponding to the emission wavelengths of 675 and 735 nm were inserted in the fluorescence path to the streak camera.

EXPERIMENTAL RESULTS AND DISCUSSION

Temperature Dependence of the Quantum Efficiency

The results shown in Fig. 1 display the quantum efficiency of bacteriorhodopsin emission (relative to the 300°K quantum efficiency) vs. temperature. Note the very strong temperature dependence of the quantum efficiency for temperatures below 150°K. The value we obtain for the 77°K relative emission intensity differs somewhat from that determined by Alfano et al. (13). We have no explanation for this dis-

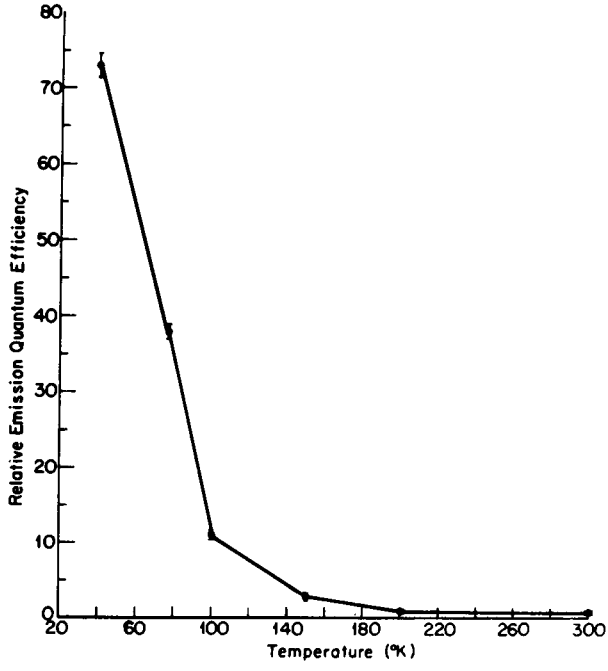

FIGURE 1 Relative emission quantum efficiency of bacteriorhodopsin (bR_{570}) vs. temperature. The quantum efficiency was computed relative to the 300°K value, $\phi_f = 1.8 \pm 1.0 \times 10^{-4}$, that is, $\phi_{rel} = \phi(T)/\phi(300°K)$.

crepancy. Furthermore, Alfano et al. (13) implicitly assume a very weak temperature dependence for the emission quantum efficiency of bacteriorhodopsin in the temperature range of 77°–90°K. Inspection of Fig. 1 shows that this assumption is in fact erroneous. This temperature region shows a very strong temperature dependence for the emission quantum efficiency.

The low temperature data points, exclusive of the 300°K measurement, may be fitted reasonably well, although possibly not uniquely, with an expression of the form:

$$\phi_{rel} = Ae^{-BT}. \quad (1)$$

Attempts to fit the observed data points to other functions of temperature (for example, an Arrhenius type equation $\phi_{rel} = Ae^{-B/T}$) did not yield reasonable results.

Temperature Dependence of the Emission Band Profiles

A variable temperature sequence of bacteriorhodopsin (bR) emission spectra is shown in Fig. 2. The spectra are similar to those reported previously (12). The 17°K spectrum has peaks at 13,900 cm^{-1} (ca 720 nm) and 12,650 cm^{-1} (ca 790 nm); a shoulder appears at 15,000 cm^{-1} (ca 670 nm). Because these features are most clearly resolved at 17°K, they are simply denoted by the above labels in what follows. The band shape does not change appreciably up to 60°K; at 100°K the intensity at 670 nm has decreased significantly, and the 720-nm peak has shifted ca 5 nm toward lower energies. The 790-nm peak is relatively unaffected. As the temperature is further in-

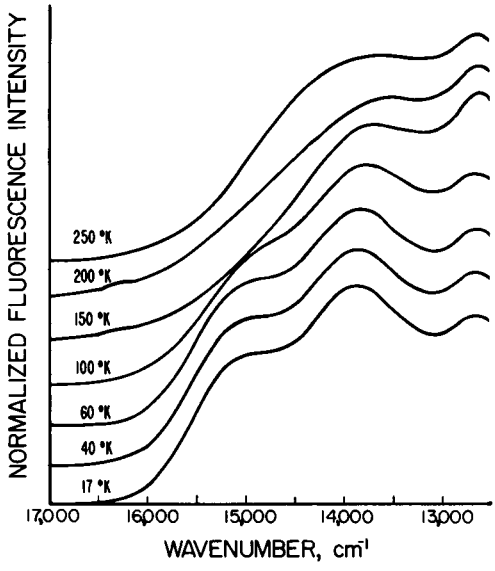

FIGURE 2 Corrected emission band profiles of bacteriorhodopsin (bR_{570}) at seven different temperatures ≤ 250°K. The areas of the spectrum at each temperature are normalized to a constant as discussed in Materials and Methods. Emission profiles at frequencies lower than 13,000 cm^{-1} may not be significant because the response of the RCA C31034 photomultiplier (RCA Solid State) is falling off rapidly in this region of the spectrum.

creased, the intensity at 680 nm continues to decrease, and the structure vanishes. A rough comparison of the normalized-area spectra for 17° and 150°K, for which the 720- to 725-nm peaks coincide, shows that the 670-nm shoulder contributes approximately half the intensity at 17°K. The 670-nm structure appears only at temperatures where bacteriorhodopsin and K_{610} are stable. Therefore the 670-nm emission cannot be due to emission from the L, M, N, or O thermal intermediates (23). Our results also indicate that the 670-nm emission is not due to the K_{610} intermediate because the single- and multiple-pulse 77°K lifetimes reported in the next section are identical, the polarization is invariant throughout both the 670- and 720-nm 77°K emission bands (12), and dual beam experiments indicate that the 670- and 720-nm spectral features arise from bacteriorhodopsin and not K_{610} (12).

Emission Lifetime and Variable Intensity Measurements

Fig. 3 shows a photographic display obtained on a single shot by the streak camera-OMA-oscilloscope detection system. The fluorescence lifetime for the entire emission spectrum of bacteriorhodopsin at 77°K and under single-pulse excitation was 60 ± 15 ps. This value was derived by averaging the lifetimes obtained from the digital information stored in the OMA (optical multichannel analyzer) for each of numerous shots taken on the best experimental run and deconvoluting by the pulse shape. This lifetime did not vary significantly with intensity over the excitation range of 5×10^{13} to 10^{15} photons/cm^2, as determined by moving a filter with attenuation of 20 at the 530-nm wavelength from the excitation beam to the fluorescence light path. Therefore, such high intensity effects as, e.g., singlet-singlet annihilation, saturation of the transition, or multiple absorption to a higher state are ruled out by the independence of lifetime with intensity, at least over this excitation range. Furthermore, the 77°K lifetimes at 670 and 735 nm are the same within experimental error as the lifetime for the entire emission spectrum. Therefore the bands observed in the emission spectrum (see Fig. 2) at 670 and 720–725 nm may arise from minima of the same electronic state.

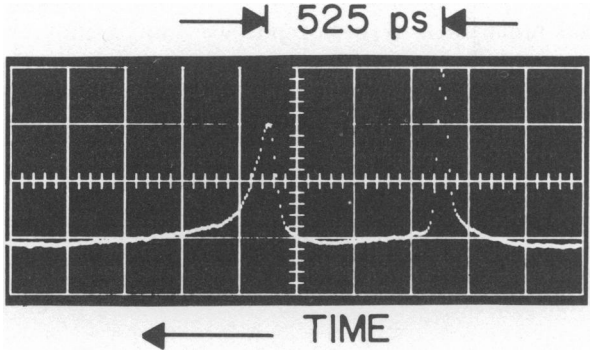

FIGURE 3 OMA-oscilloscope display of fluorescent streak from bacteriorhodopsin at 77°K excited with a single 530-nm pulse. Calibration pulse at right of display travels along a separate path arriving 525 ps before the fluorescence from the sample.

No variation of the lifetime was observed when the sample was subjected to light from a slide projector with a sample temperature of 77°K.

Because the 60-ps lifetime at 77°K is somewhat longer than obtained previously, and because of the wide differences in lifetime between the two earlier measurements with pulse trains at room temperature, we also performed a lifetime measurement with a pulse train. With a pulse train consisting of about 10 intense pulses separated by 6 ns, the fluorescence lifetime observed from the fifth excitation pulse was not affected by the four preceding pulses with excitation intensities as high as 10^{15} photons/cm^2 per pulse. Thus, the buildup of any extraneous state, such as a triplet or other intermediate, did not affect the fluorescence over a period of roughly 20 ns. This is particularly significant because triplet formation is very efficient in all *trans*-retinal (24; although not in protonated Schiff bases [25]) and because pulse-train effects, such as generation of intermediates, partially account for varying results in dyes (e.g., DODCI (3,3′-diethyloxadi carbocyanine iodide) [26–28]), in photosynthetic systems (e.g., *Chlorella* and spinach chloroplasts [21, 22, 29, 30]), and in scintillators (e.g., NE102 Nuclear Enterprises 102, (Nuclear Enterprises (G.B.) Ltd., Edinburgh, Scotland)).[1] Thus, even though 100–1,000 excitation pulses were used in previous measurements, and the batho intermediate of bacteriorhodopsin is formed in a picosecond, it appears unlikely that differences between previous measurements can be explained in terms of pulse-train effects even though their pulse trains were very long.

As a further test for possible intensity effects, the relative quantum efficiency was measured as a function of intensity at both room and low temperature for single-pulse excitation. Room and low temperature data show that the quantum efficiency curve is flat over the intensity range 10^{12}–10^{15} photons/cm^2, further confirming that the lifetime should not vary over this excitation range. Although an apparent decrease in quantum efficiency is noted for the room temperature sample at very high intensities, the value of 4×10^{15} photons/cm^2 at which the quantum efficiency declines to 0.7 of its low intensity limit, is more than 10 times higher than the intensity quoted by Hirsch et al. (14) and 6.7 times higher than that quoted by Alfano et al. (13). Thus, such high values could have been reached in prior experiments only if parameters such as peak pulse intensity, peak radial intensity, or hot spots were not carefully considered.

At room temperature the observed decrease in quantum efficiency above 10^{15} photons/cm^2 could be on account of numerous nonlinear factors because a large fraction of the molecules is excited. However, singlet-singlet annihilation observed in a number of other systems (14, 31, 32) is an unlikely explanation because of the poor overlap between the absorption and emission bands in bacteriorhodopsin. Also assuming identical physical mechanisms to reach the exciton level at both room and low temperatures, in singlet-singlet annihilation the relative quantum efficiency, ϕ, as a function of excitation intensity, I, would follow the form $\phi/\phi_0 = (k/\Gamma I) \ln (1 + \Gamma I/k)$,

[1] Campillo, A. J., P. Lyons, S. L. Shapiro, and K. R. Winn. Manuscript submitted for publication.

where ϕ_0 is the quantum efficiency at low intensity, k is the radiative rate, and Γ is the exciton annihilation coefficient (33). If the exciton annihilation rate remained reasonably constant with temperature, as expected, and if k, again as expected, would change by a large factor of $\simeq$38) because of differences in quantum efficiency at 77°K and room temperatures, the simple formula would predict a shift of the curve toward low intensities by a factor of roughly 38. No such shift is observed. Therefore, because the absorption cross-section per molecule is of the order of an angstrom square at 530 nm, the decrease is apparently due to a saturation type of effect.

In an attempt to measure the lifetime at room temperature, very weak emission was detected with very high incident intensity (5×10^{14} to 10^{15} photons/cm^2). Streak camera measurements show that the lifetime for this emission appeared to be resolution limited, i.e., $\leq$ 20 ps. This result is consistent with earlier pulse-train measurements (12–14). Provided that the emitting level is fed at the same rate at 77° and 300°K, the fluorescence lifetime at room temperature may be estimated by dividing our value for the fluorescence lifetime at 77°K, 60 ps, by the relative quantum efficiencies at 77° and 300°K. By basing our estimate on our new relative quantum yield measurements (38 to 1), we arrive at a value of 1.5±0.4 ps for the estimated lifetime at room temperature. It is interesting that this coincides with the value of 1.0±0.4 ps observed by Ippen et al. (11) for the formation time of a new state observed in absorption. The agreement therefore may be indicative of a relatively uncomplicated model. (Note that although Alfano et al. [13] estimated a lifetime of 3 ps based on quantum yield data, their measurement of 40±5 ps at 90°K yields an estimate of 1.7±0.2 ps at room temperature if the value of 24, obtained in this paper, is used for the relative increase in quantum yield between 90°K and room temperature. Note, also, that all the low temperature lifetime data are in agreement if the quantum yield data in Fig. 1 are used for comparison.) Thus, all the low temperature emission lifetime data and our variable temperature emission quantum efficiency results suggest that a 1.4±0.5-ps emitting minimum does exist at room temperature.

Previous measurements at room temperature of fluorescence emission by Hirsch et al. (14), using an up-conversion gate, pulse-train excitation, and 10-ps pulse durations that detected a 15-ps lifetime, and an absorption measurement by Kaufmann et al. (7) using a high intensity single-pulse excitation of $\simeq$6-ps duration that detected a $\simeq$15-ps transient at 580 nm would require more complex interpretation which at this point could not be definitive. More measurements are needed to tie all the results together. Subpicosecond fluorescence experiments as well as subpicosecond absorption experiments (at a variety of wavelengths) should be performed at room and low temperatures.

We would like to thank Dr. C. E. Swenberg for helpful discussions and K. R. Winn for technical assistance.

This work was supported by the U.S. Department of Energy and by a National Institutes of Health grant to A.L. (no. EY01 377).

Received for publication 23 January 1978.

REFERENCES

1. OESTERHELT, D., and W. STOECKENIUS. 1971. Rhodopsin-like protein from the purple membrane of *Halobacterium halobium*. *Nat. New Biol.* **233**:149–152.
2. OESTERHELT, D., and W. STOECKENIUS. 1973. Functions of a new photoreceptor membrane. *Proc. Natl. Acad. Sci. U. S. A.* **70**:2853–2857.
3. LEWIS, A., J. P. SPOONHOWER, R. A. BOGOMOLNI, R. H. LOZIER, and W. STOECKENIUS. 1974. Tunable laser resonance Raman spectroscopy of bacteriorhodopsin. *Proc. Natl. Acad. Sci. U. S. A.* **71**:4462–4466.
4. MARCUS, M. A., and A. LEWIS. 1977. Kinetic resonance Raman spectroscopy: dynamics of the deprotonation of the Schiff base of bacteriorhodopsin. *Science (Wash. D. C.).* **195**:1328–1330.
5. STOECKENIUS, W., and R. H. LOZIER. 1974. Light energy conversion in *Halobacterium halobium*. *J. Supramol. Struct.* **2**:769–775.
6. LOZIER, R. H., R. A. BOGOMOLNI, and W. STOECKENIUS. 1975. Bacteriorhodopsin: a light-driven proton pump in *Halobacterium Halobium*. *Biophys. J.* **15**:955–962.
7. KAUFMANN, K. J., P. M. RENTZEPIS, W. STOECKENIUS, and A. LEWIS. 1976. Primary photochemical processes in bacteriorhodopsin. *Biochem. Biophys. Res. Commun.* **68**:1109–1115.
8. BUSCH, G. E., M. L. APPLEBURY, A. A. LAMOLA, and P. M. RENTZEPIS. 1972. Formation and decay of prelumirhodopsin at room temperatures. *Proc. Natl. Acad. Sci. U. S. A.* **69**:2802–2806.
9. LEWIS, A. 1977. Primary processes in visual transduction. *In* Electrical Phenomena at the Membrane Level. E. Roux, editor. Elsevier, Amsterdam. 543–563.
10. ROSENFELD, T., B. HONIG, M. OTTOLENGHI, J. HURLEY, and T. G. EBREY. 1977. Cis trans isomerization in the photochemistry of vision. *Pure Appl. Chem.* **49**:341–351.
11. IPPEN, E. P., C. V. SHANK, A. LEWIS, and M. A. MARCUS. 1978. Subpicosecond spectroscopy of bacteriorhodopsin. *Science (Wash. D. C.).* **200**:1279–1281.
12. LEWIS, A., J. P. SPOONHOWER, and G. J. PERREAULT. 1976. Observation of light emission from a rhodopsin. *Nature (Lond.).* **260**:675–678.
13. ALFANO, R. R., W. YU, R. GOVINDJEE, B. BECHER, and T. G. EBREY. 1976. Picosecond kinetics of the fluorescence from the chromophore of the purple membrane protein of *Halobacterium halobium*. *Biophys. J.* **16**:541–545.
14. HIRSCH, M. D., M. A. MARCUS, A. LEWIS, H. MAHR, and N. FRIGO. 1976. A method for measuring picosecond phenomena in photolabile species. *Biophys. J.* **16**:1399–1409.
15. OESTERHELT, D., and W. STOECKENIUS. 1974. Isolation of the cell membrane of *Halobacterium halobium* and its fractionation into red and purple membrane. *Methods Enzymol.* **31A**:667–678.
16. CLAYTON, R. K., and R. T. WANG. 1971. Photochemical reaction centers from *Rhodopseudomonas Sphaeroides*. *Methods Enzymol.* **23A**:696–704.
17. ZANKEL, K. L., D. W. REED, and R. K. CLAYTON. 1968. Fluorescence and photochemical quenching in photosynthetic reaction centers. *Proc. Natl. Acad. Sci. U. S. A.* **61**:1243–1249.
18. GILLBRO, T., A. N. KRIEBEL, and U. P. WILD. 1977. On the origin of the red emission of light adapted purple membrane of *Halobacterium halobium*. *FEBS (Fed. Eur. Biochem. Soc.) Lett.* **78**:57–60.
19. PERREAULT, G. J., R. E. COOKINGHAM, J. P. SPOONHOWER, and A. LEWIS. 1976. A single channel printing scalar for photon counting. *Appl. Spectrosc.* **30**:614–620.
20. SAVITZKY, A., and M. J. E. GOLAY. 1964. Smoothing and differentiation of data by simplified least squares procedures. *Anal. Chem.* **36**:1627–1639.
21. CAMPILLO, A. J., S. L. SHAPIRO, V. H. KOLLMAN, K. R. WINN, and R. C. HYER. 1976. Picosecond exciton annihilation in photosynthetic systems. *Biophys. J.* **16**:93–97.
22. CAMPILLO, A. J., V. H. KOLLMAN, and S. L. SHAPIRO. 1976. Intensity dependence of the fluorescence lifetime of *in vivo* chlorophyll excited by a picosecond light pulse. *Science (Wash. D. C.).* **193**:227–229.
23. GILLBRO, T., and A. N. KRIEBEL. 1977. Emission from secondary intermediates in the photocycle of bacteriorhodopsin at 77°K. *FEBS (Fed. Eur. Biochem. Soc.) Lett.* **79**:29–32.
24. HOCHSTRASSER, R. M., D. L. NARVA, and A. C. NELSON. 1976. Picosecond photophysics of *trans*-retinal. *Chem. Phys. Lett.* **43**:15–19.
25. FISHER, M. M., and K. WEISS. 1974. Laser photolysis of retinal and its protonated and unprotonated *n*-butylamine Schiff base. *Photochem. Photobiol.* **20**:423–432.
26. SHANK, C. V., and E. P. IPPEN. 1975. Anisotropic absorption saturation with picosecond pulses. *Appl. Phys. Lett.* **26**:62–63.

27. MAGDE, D., and M. W. WINDSOR. 1974. Picosecond flash photolysis and spectroscopy: DODCI. *Chem. Phys. Lett.* **27**:31–36.
28. MIALOCQ, J. C., A. W. BOYD, J. JARAUDIAS, and J. SUTTON. 1976. Fluorescence lifetimes of DODCI excited by single and multiple picosecond pulses. *Chem. Phys. Lett.* **37**:236–239.
29. PORTER, G., J. A. SYNOWIEC, and C. J. TREDWELL. 1977. Intensity effects on the fluorescence lifetime of *in vivo* chlorophyll. *Biochim. Biophys. Acta.* **459**:329–336.
30. GEACINTOV, N. E., J. BRETON, C. E. SWENBERG, A. J. CAMPILLO, R. C. HYER, and S. L. SHAPIRO. 1977. Picosecond and microsecond pulse laser studies of exciton quenching and exciton distribution in spinach chloroplasts at low temperature. *Biochim. Biophys. Acta.* **461**:306–312.
31. CAMPILLO, A. J., R. C. HYER, S. L. SHAPIRO, and C. E. SWENBERG. 1977. Exciton interactions in crystalline tetracene studied by single picosecond pulse excitation. *Chem. Phys. Lett.* **48**:495–500.
32. CAMPILLO, A. J., R. C. HYER, T. G. MONGER, W. W. PARSON, and S. L. SHAPIRO. 1977. Light collection and harvesting processes in bacterial photosynthesis investigated on a picosecond time scale. *Proc. Natl. Acad. Sci. U. S. A.* **74**:1997–2001.
33. SWENBERG, C. E., N. E. GEACINTOV, and M. POPE. 1976. Bimolecular quenching of excitons and fluorescence in the photosynthetic unit. *Biophys. J.* **16**:1447–1452.